NATIONAL ADVISORY COMMITTEE FOR AERONAUTICS

TECHNICAL NOTE 4210

STABILITY OF PROPANE-AIR FLAMES IN VORTEX FLOW

By A. E. Potter, Jr., E. L. Wong, and A. L. Berlad

Lewis Flight Propulsion Laboratory
Cleveland, Ohio

Washington
February 1958

NATIONAL ADVISORY COMMITTEE FOR AERONAUTICS

TECHNICAL NOTE 4210

STABILITY OF PROPANE-AIR FLAMES IN VORTEX FLOW

By A. E. Potter, Jr., E. L. Wong,
and A. L. Berlad

SUMMARY

A vortex burner in which the vortex strength could be varied at constant flow rate was used for a study of propane-air vortex flames. The effect of weak vortices on a Bunsen flame was to distort the flame shape slightly. Strong vortices caused the flame to assume an inverted cone shape. Since this flame did not touch the burner, it was stabilized by a different mechanism from an ordinary Bunsen flame. The stability limits of propane-air flames in strong vortices were measured. The blow-off velocity varied to the 0.73 power of vortex strength and increased slightly with fuel concentration at constant vortex strength. Reverse flow was observed in both cold flow and in flames. It appears that flames in strong vortices are stabilized by a stagnation or near-stagnation region induced by a pressure defect at the vortex center. When the vortex strength was made large, the pressure defect at the vortex center drew ambient air into the flame. This causes partial quenching of lean flames. Hydrogen peroxide, formaldehyde, higher aldehydes, methanol, hydrogen, and carbon monoxide were found in the combustion products of lean flames in strong vortices.

INTRODUCTION

Hottel and Person (ref. 1) studied flames stabilized in vortex flow in the hope of discovering a combustion system of improved stability and mixing properties. They predicted and observed a recirculation zone along the vortex axis induced by the vortex flow. However, their system for producing the flow did not yield a significant amount of recirculation; thus, no definite conclusions were reached. Albright and Alexander (ref. 2) improved the system of producing vortex flow and obtained strong recirculation along the stream axis. They found that the recirculation zone made the flame very stable. They also observed incomplete combustion in fuel-lean flames in strong vortices. Kurz (refs. 3 to 5) has done considerable work on the effect of fuel type on the stability of vortex flames. Moore and Martin (ref. 6) have published some observations on flames in vortex flow. The apparatus of all these investigators

was so designed that the strength of the vortex was a function of flow rate through the apparatus. Consequently, the effects of varying vortex strength at constant flow rate could not be observed.

In the apparatus to be described, the vortex strength also is a function of flow rate, but can be varied independently. This report gives an account of the behavior of flames in vortex flow when the strength of the vortex is varied at constant flow rate. A discussion of the flow patterns in the apparatus and the effect of the flow on flames are given. Included herein are studies of the stability limits of vortex flames, a discussion of the mechanism by which these flames are stabilized, and some observations and measurements on incomplete combustion in fuel-lean vortex flames.

APPARATUS

The vortex burner is shown schematically in figure 1. It consisted of a large tube containing a rotating cylindrical centerbody; the entire apparatus was capped by a converging nozzle. Gas was made to flow through the annular space between the outer stationary cylinder and the inner rotating centerbody. The angular velocity of the gas was controlled by the speed of the centerbody. After passage through the annular space, the gas was directed through the converging nozzle. Flames were stabilized at the nozzle exit. The nozzle was water cooled and had a diameter of 1/2 inch at the exit. The spinning centerbody had a diameter of 2.36 inches, and the stationary Pyrex glass cylinder which surrounded it had a diameter of 3.00 inches, so that the annular space between the two was 0.32 inch. The rotational speed of the centerbody was measured by a magnetic pickup system and could be varied from 0 to 3200 rpm by means of a Vickers Hydraulic Transmission. Fuel (propane) and air were metered by critical-flow orifices. Turbulence-intensity and stream-velocity measurements were made with a constant-temperature hot-wire anemometer. Static pressure at the nozzle axis at the end of the converging section of the nozzle (1.3 cm upstream of the nozzle exit) was measured with a 0.02-inch outside-diameter tube attached to a micromanometer. The experimental arrangement is shown in figure 2. The pressure difference between the tube end at the nozzle axis and the atmosphere was zero at all flow velocities with the centerbody motionless. The pressure at the nozzle axis ranged from 0.001 to 0.040 inch of water below atmospheric pressure with the centerbody turning.

FLOW IN APPARATUS

A general understanding of the flow was gained by observation of the patterns produced by smoke blown through the apparatus. Three distinct types of gas motion were observed as illustrated in figure 3. The

dominant motion at all centerbody speeds is cyclonic. At low rotational speeds, this is the only type of motion present. At higher speeds, some circular, or "smoke ring," vortices appear. At still higher speeds, turbulence sets in and the circular vortices disappear. The appearance of the circular vortices is a well-known phenomenon and is discussed in reference 7. If circular vortices and turbulence are neglected for the moment because of their minor effects on the flame, the flow at the nozzle can be thought of as the superposition of two flows. One is vortex flow in which the gas travels in circles the center of which is the nozzle axis. The other is axial flow in which the gas travels in straight lines parallel to the nozzle axis. If the hot-wire anemometer did not respond to flow parallel to its axis, it could be used for accurate measurement of these velocity components. Axial velocities could be measured by placing the hot wire tangent to circles whose centers are the nozzle axis. Vortex velocities could be measured by placing the hot wire parallel to the nozzle axis. Unfortunately, the hot wire does respond to flow parallel to its axis (caused largely by the wire supports), and such measurements are quite inaccurate. Even so it is informative to look at vortex and axial velocities measured by this method for the purpose of illustrating qualitatively the effects of centerbody rotation on the flow. Some representative vortex- and axial-velocity profiles downstream of the nozzle exit are shown in figure 4. From this figure, it can be seen that the vortex flow has two parts. Close to the nozzle axis the velocity increases with increasing distance from the nozzle axis. Near the nozzle perimeter, the velocity decreases with increasing distance from the nozzle axis. This is the normal flow pattern characteristic of a rectilinear vortex in an infinite fluid at rest (ref. 8). In vortex flow, the pressure decreases as the axis is approached. Since the pressure at the perimeter of the vortex is atmospheric, the pressure must be below atmospheric at the vortex center. However, far downstream of the nozzle, the pressure is everywhere constant and equal to atmospheric pressure. Consequently, a pressure gradient exists that tends to produce flow in the upstream direction along the axis. The pressure gradient is largest at the nozzle axis. As a result the flat axial-velocity profile at the nozzle exit, obtained with no cyclonic motion, becomes distorted to the shape shown in figure 4(b) when cyclonic motion is present. When the vortex becomes strong enough, the pressure gradient down along the axis becomes large enough to induce reverse flow along the axis. The reverse flow guarantees that at some point along the axis a stagnant region will exist in which a flame can stabilize.

The occurrence of reverse flow at the axis is shown in figure 5, where flow velocity at the nozzle axis is plotted against centerbody speed. Velocity out of the nozzle is given a positive sign and velocity into the nozzle is given a negative sign. The magnitude of the velocity was measured with the hot-wire anemometer. The direction of flow was determined by introducing smoke into the flow. Figure 5 shows that, as the

vortex strength is increased by increasing the centerbody speed, the flow velocity at the nozzle axis becomes smaller, becomes zero at about 180 rpm, and then reverses direction at higher centerbody speeds.

The point at which reverse flow ceases (the stagnation point) was observed to move downstream along the nozzle axis with decreasing centerbody speed, and upstream with increasing centerbody speed.

Measurement of Vortex Strength

In order to draw some conclusions concerning the effect of vortex flow on flames, it is necessary to characterize the vortex flow. The vortex strength was chosen for this purpose. Either the angular velocity or the pressure defect at the vortex axis could have been chosen equally as well, since all these vortex properties are closely related, as shown below.

The strength of a vortex $\varkappa$ is defined as (ref. 8)

$$\varkappa = \frac{1}{2}\omega a^2 \tag{1}$$

where ω is the angular velocity and a is the radius of the vortex tube. The vortex strength is analogous to the source strength in that it is a velocity multiplied by an area. The vortex strength can easily be calculated from the static pressure at the vortex axis, since it may be shown that

$$\Delta P = \frac{\varkappa^2 \rho}{a^2} \tag{2}$$

where ΔP is the difference between ambient pressure and pressure at the vortex axis and ρ is the density of the fluid. The vortex strength in the apparatus was determined as a function of centerbody speed and flow velocity from static-pressure measurements at the vortex axis. The static pressure for the calculation of vortex strength was measured near the end of the converging section of the nozzle (about 1.3 cm below the nozzle exit). Measurements at higher points gave smaller strengths, possibly because of recirculation along the nozzle axis. The results are shown in figure 6 in which vortex strength at three flow rates is plotted against centerbody speed. The vortex strength varies nearly linearly with flow velocity and is much more affected by it than by centerbody speed.

Turbulence

The root-mean-square turbulent velocity was measured at various points across the nozzle exit by multiplying the percentage of turbulence and the flow velocity as measured by the hot-wire anemometer. An example of the results is shown in figure 7. Because the turbulence is certainly anisotropic, the results shown in figure 7 only serve to show that turbulence does exist and is distributed in a manner similar to vortex velocity.

4680

FLAMES IN VORTEX FLOW

Figure 8 illustrates the changes in appearance of a flame stabilized above the nozzle as the vortex strength is increased by increasing the speed of the centerbody. When the centerbody is motionless, a laminar flame of normal conical shape is obtained (fig. 8(a)). When the centerbody begins to turn slowly, the vortex flow causes the top of the flame to assume a twisted corkscrew-like shape (fig. 8(b)). Further increase in the speed of the centerbody makes the vortex strong enough to alter the axial-velocity profile across the nozzle part of the shape shown in figure 4(b). As a result, the upper part of the flame cone becomes inverted (fig. 8(c)). As the vortex becomes stronger, the axial velocity at the nozzle rim becomes so large that the critical boundary velocity gradient for blowoff is exceeded, and the flame is lifted off the rim. The flame then becomes a completely inverted cone (fig. 8(d)). In most cases, reverse flow along the axis has set in, and these flames usually have recirculation zones. The smoke-ring vortices did not seem to affect the flame, although occasional sudden movements of the flame up and down were observed that might have been caused by these vortices. Further increases in centerbody speed produce turbulence, which is reflected in the brushy appearance of the flame (fig. 8(e)). At very high centerbody speeds, unusual differences between the appearance of rich and lean flames are observed. The fuel-rich flame in strong vortices (fig. 8(f)) consists of a long, dim, green recirculation zone extending far down the nozzle, surrounded by a bright blue, fiercely burning halo of turbulent flames. As centerbody speed is increased the flame burns more vigorously. The fuel-lean flame in strong vortices (fig. 8(g)) is very dim, pale blue, has a very strong recirculation zone, and emits aldehydes and other products of partial combustion. The tip of the flame projects a short distance into the nozzle, but apparently does not extend to the top of the centerbody as does the fuel-rich flame (fig. 8(f)). The top of the centerbody was visible through the glass outer tube. No flame could be observed there for the fuel-lean flame (fig. 8(g)) even in a darkened room. As centerbody speed is increased, the flame becomes dimmer and the odor of aldehydes becomes stronger. Further increases of centerbody speed quench the flame entirely. Albright and Alexander (ref. 2) have also observed partial combustion in lean vortex flames. Because the production of aldehydes by a fuel-lean flame is very unusual, the flame shown in figure 8(g) was investigated in detail.

The Fuel-Lean Vortex Flame

The first experiment performed with the fuel-lean flame in a very strong vortex was to surround it with a large glass tube to prevent the access of atmospheric air. The experimental arrangement is shown in figure 9. When this was done, the flame spread out and filled the entire tube. Simultaneously, the odor of aldehydes disappeared. Furthermore, the flame was stable at centerbody speeds in excess of 2000 rpm. Thus, the incomplete combustion observed in this flame is apparently caused by rapid quenching or chilling of the flame by admixture with ambient air. This also explains the bright and vigorous appearance of the fuel-rich flame, since in this case, the admixture of air makes the flame more vigorous.

The temperature of the gases in the recirculation zone of the fuel-lean flame was measured as a function of vortex strength by a sodium-line reversal technique. The results are shown in figure 10. The temperature is seen to decrease rapidly as the centerbody speed, that is, the vortex strength, increases. This must mean that the amount of cold ambient air brought into the recirculation zone increases with vortex strength. It is significant to note that the temperature at which the flame disappears is near the lean-limit flame temperature.

To complete the study of this flame, samples of the combustion products were analyzed. Samples were withdrawn by a water-cooled probe from two places in the flame, the recirculation zone and the edge of the flame. The hot gases from the flame were drawn through a cold trap held at dry-ice temperature. In this way, the combustion products were separated into two parts, the condensable and the noncondensable. The condensable fraction was mostly water, and was analyzed by standard methods for entrained hydrogen peroxide, formaldehyde, higher aldehydes, and methanol. The noncondensable fraction was analyzed for oxygen, nitrogen, carbon monoxide, carbon dioxide, hydrogen, and hydrocarbon (calculated as CH_4) by standard methods. The over-all composition of the combustion products was calculated from the analytical results and is shown in table I. It may be seen from this table that combustion is less complete at the upper edge of the flame than in the recirculation zone. This would appear to indicate that the flame is quenched by mixing with ambient air at the edge of the flame. In addition, the analytical results can be used to calculate the ratio of total carbon to total oxygen in the combustion products. This ratio is smaller than the carbon-oxygen ratio in the unburned combustible mixture, indicating that air has been mixed into the combustion products.

The amounts of combustion intermediates found were small. However, the vortex strength was kept relatively low for the flame that was sampled, since the sampling probe made the flame very unstable at high vortex strengths. At high vortex strengths, much greater amounts of intermediate combustion products were formed, as evidenced by the overpowering odor of formaldehyde produced in a very short time.

Stability of Vortex Flames

When the vortex is weak, its only effect on flame is to distort the flame shape as shown in figure 8(b). The flame is anchored at the burner lip in the same way as a normal Bunsen flame. However, as the vortex is made strong, the flame becomes an inverted cone, nowhere touching the burner. Clearly, a different mechanism of flame stabilization is operative in strong vortices.

In strong vortices, reverse flow along the axis occurs as discussed previously and terminates at a stagnation point on the axis. The flame is apparently stabilized at or near this point as evidenced by, first, flames in strong vortices show reverse flow behind the flame front in the combustion products. The existence of reverse flow was shown by inserting a salt-tipped wire into the flame. The yellow-glowing gases produced by vaporization of salt from the wire were swept upstream if reverse flow existed. The region of reverse flow (the recirculation zone) had a very definite length, which varied with fuel concentration at constant vortex strength and flow rate. In lean and rich flames the recirculation zone was about 1 centimeter long. In near-stoichiometric flames the recirculation zone became so short that it was impossible to distinguish between reverse flow and diffusion of sodium vapor upstream of the wire.

Second, the flame position moves along the nozzle axis in the same way the stagnation point does when vortex strength is changed. Stability limits for flames in strong vortices are shown in figures 11(a) to (e). It can be seen from these figures that as the centerbody speed (i.e., the vortex strength) is decreased at constant flow rate, the flame moves downstream. When it moves too far downstream, it becomes unsteady and eventually blows off. When centerbody speed is increased, the flame moves in the opposite direction, upstream into the nozzle. When it reaches the low velocity region inside the nozzle, it flashes back through the annular space. Flashback is a phenomenon peculiar to this apparatus. Had the vortex flow been produced by tangential vanes or other such devices, flashback would not occur, rather, the flame would simply move closer to the vortex-producing device as the vortex strength increased. On the other hand, blowoff is a phenomenon common to all vortex burners. If the existence of a flame on the vortex burner rests mainly upon the presence of a stagnation point not too far downstream of the nozzle exit, the stability of the flame, that is, its blowoff velocity, should depend principally upon the vortex strength. This is the case, as seen in figure 12 in which blowoff velocity at several fuel concentrations is plotted against vortex strength. The points shown in figure 12 were obtained from cross plots of figures 6 and 11. The effect of fuel concentration is small enough that it seems reasonable to draw a single line through the data points. From the slope and intercept of this line, it is found that the functional relation between blowoff velocity V_{bo} and vortex strength $\varkappa$ is

$$V_{bo} = 8.3\varkappa^{0.73} \tag{3}$$

It seems likely that the essential feature in vortex flame stabilization is not so much the stagnation zone, but the velocity gradient along the nozzle axis which must be associated with it. This gradient is normal to the flame front. The flame moves upstream against this gradient until the flow velocity equals the burning velocity. Thus, the stagnation zone is not necessary if the axial velocity gradient exists. As a result, the flame can be stabilized by a near-stagnation zone if a large enough axial velocity gradient is associated with it. To examine more closely the small effect that fuel concentration has on blowoff velocity, figure 13 was constructed from the data shown in figures 6 and 11. Figure 13 is a plot of fuel concentration against blowoff velocity at constant vortex strength. The blowoff velocity increases with fuel concentration φ. The increase in blowoff velocity from $\varphi = 0.7$ to $\varphi = 1.1$ is about the same as the increase in burning velocity. Kurz (refs. 3 to 5) has presented observations concerning the effect of fuel type on blowoff of vortex flames, which indicate that blowoff velocity increases with burning velocity.

CONCLUDING REMARKS

The possibility exists that a bluff body and a vortex generator might be combined to give a flameholder of superior quality. Such a flameholder would consist of a series of vanes arranged in the manner of a windmill. Flow through this flameholder would produce vortex flow. Spinning the flameholder will increase the vortex strength and the flameholding efficiency. Scurlock (ref. 9) has demonstrated that a spinning rod is an effective flameholder and flame spreader. It seems possible that the properties of his spinning flameholder could be improved by designing it according to the observations outlined.

SUMMARY

Flames in strong vortices are stabilized by a region of stagnant or near-stagnant flow induced by a pressure defect at the vortex center. As a result, the blowoff velocity depends primarily on the vortex strength. However, blowoff velocity increases slightly with fuel concentration, probably because of increased burning velocity. Incomplete combustion of fuel-lean propane-air flames in strong vortices is caused by rapid chilling of the burning gases by the admixture of ambient air. Among the products of incomplete combustion are carbon monoxide, hydrogen, hydrogen peroxide, formaldehyde, hydrocarbons, higher aldehydes, and methanol.

Lewis Flight Propulsion Laboratory
National Advisory Committee for Aeronautics
Cleveland, Ohio, November 8, 1957

REFERENCES

1. Hottel, H. C., and Person, R. A.: Heterogeneous Combustion of Gases in a Vortex System. Fourth Symposium (International) on Combustion, The Williams & Wilkins Co., 1953, pp. 781-788.

2. Albright, Lyle F., and Alexander, Lloyd G.: Stable Cyclonic Flames of Natural Gas and Air. Jet Prop., vol. 26, no. 10, Oct. 1956, pp. 867-873.

3. Kurz, Philip F.: Flame Studies with a Vortex Burner. Ind. and Eng. Chem., vol. 46, no. 6, June 1954, pp. 1311-1314.

4. Kurz, Philip F.: Flame Stability Studies with Hydrocarbon Mixtures. Fuel, vol. 34, no. 3, July 1955, pp. 269-282.

5. Kurz, Philip F.: Behavior of Diborane and Propane-Diborane Flames on a Vortex Burner. Fuel, vol. 35, no. 3, July 1956, pp. 318-322.

6. Moore, N. P. W., and Martin, D. G.: Flame Propagation in Vortex Flow. Fuel, vol. 32, 1953, pp. 393-394.

7. Taylor, G. I.: Stability of a Viscous Liquid Contained Between Two Rotating Cylinders. Phil. Trans. Roy. Soc. (London), ser. A, vol. 223, 1923, pp. 289-343.

8. Milne-Thomson, L. M.: Theoretical Hydrodynamics. MacMillan and Co., Ltd. (London), 1938, p. 318.

9. Grover, J. H., Kesler, M. G., and Scurlock, A. C.: Rotating Flame Stabilizer. Jet Prop., vol. 27, no. 4, Apr. 1957, pp. 386-391.

TABLE I. - COMPOSITION OF COMBUSTION PRODUCTS

FROM LEAN (3.1 PERCENT C_3H_8)

PROPANE-AIR VORTEX FLAME

[Flow velocity, 396 cm/sec;

centerbody speed, 443 rpm]

Component	Percent at upper edge of flame	Percent at recirculation zone
H_2	0.8	0.2
Hydrocarbon (As CH_4)	.5	.03
CO_2	3.9	7.7
CO	1.3	.1
O_2	13.4	7.7
N_2	75.2	74.6
H_2O	4.9	9.7
HCHO	5×10^{-4}	1.3×10^{-4}
Other aldehydes	1.8×10^{-3}	1.7×10^{-4}
H_2O_2	2.4×10^{-7}	1.3×10^{-6}
CH_3OH	6.0×10^{-4}	7.0×10^{-5}

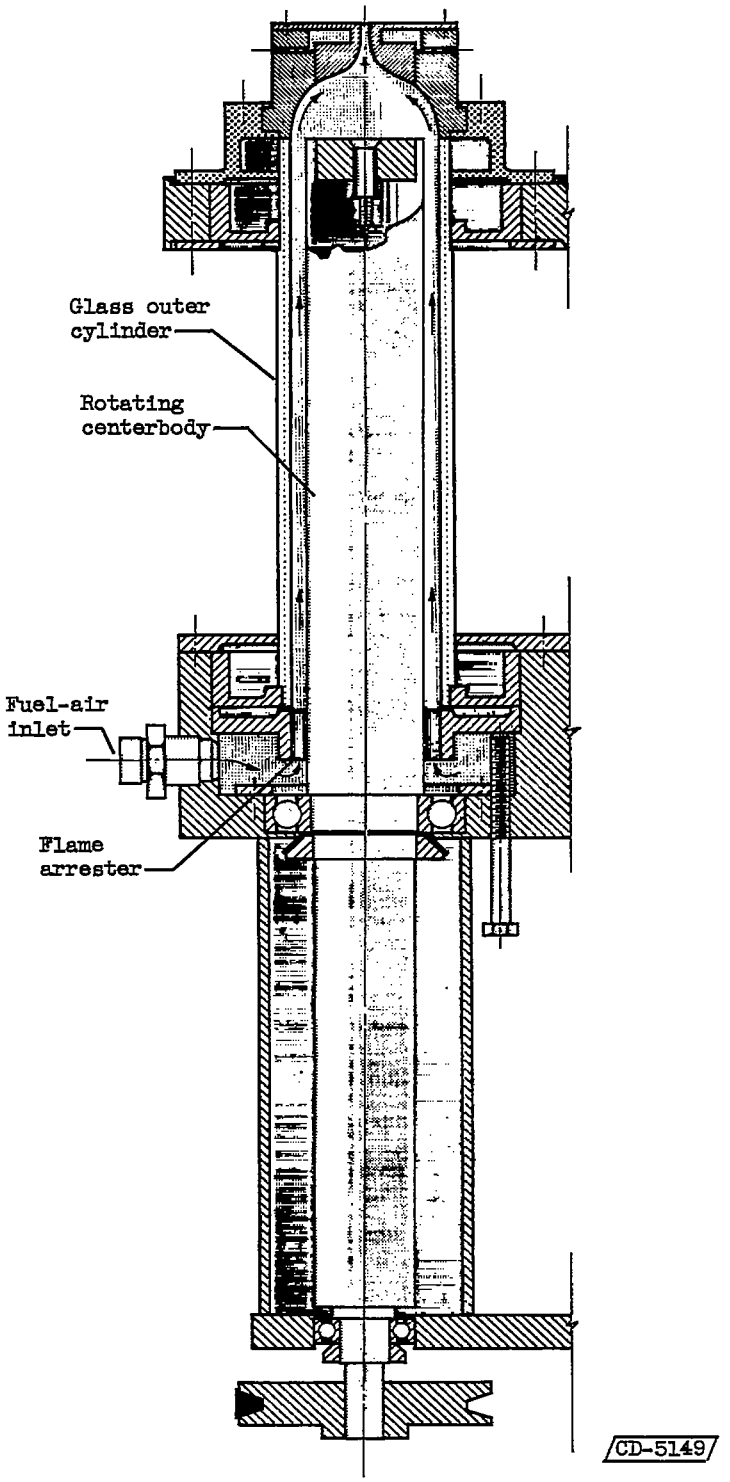

Figure 1. - Vortex burner.

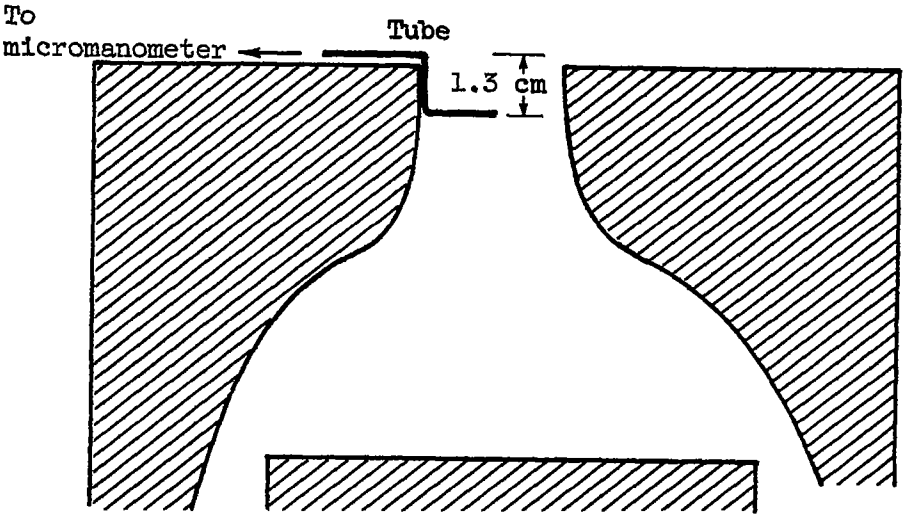

Figure 2. - Experimental arrangement for measuring pressure defect at nozzle axis.

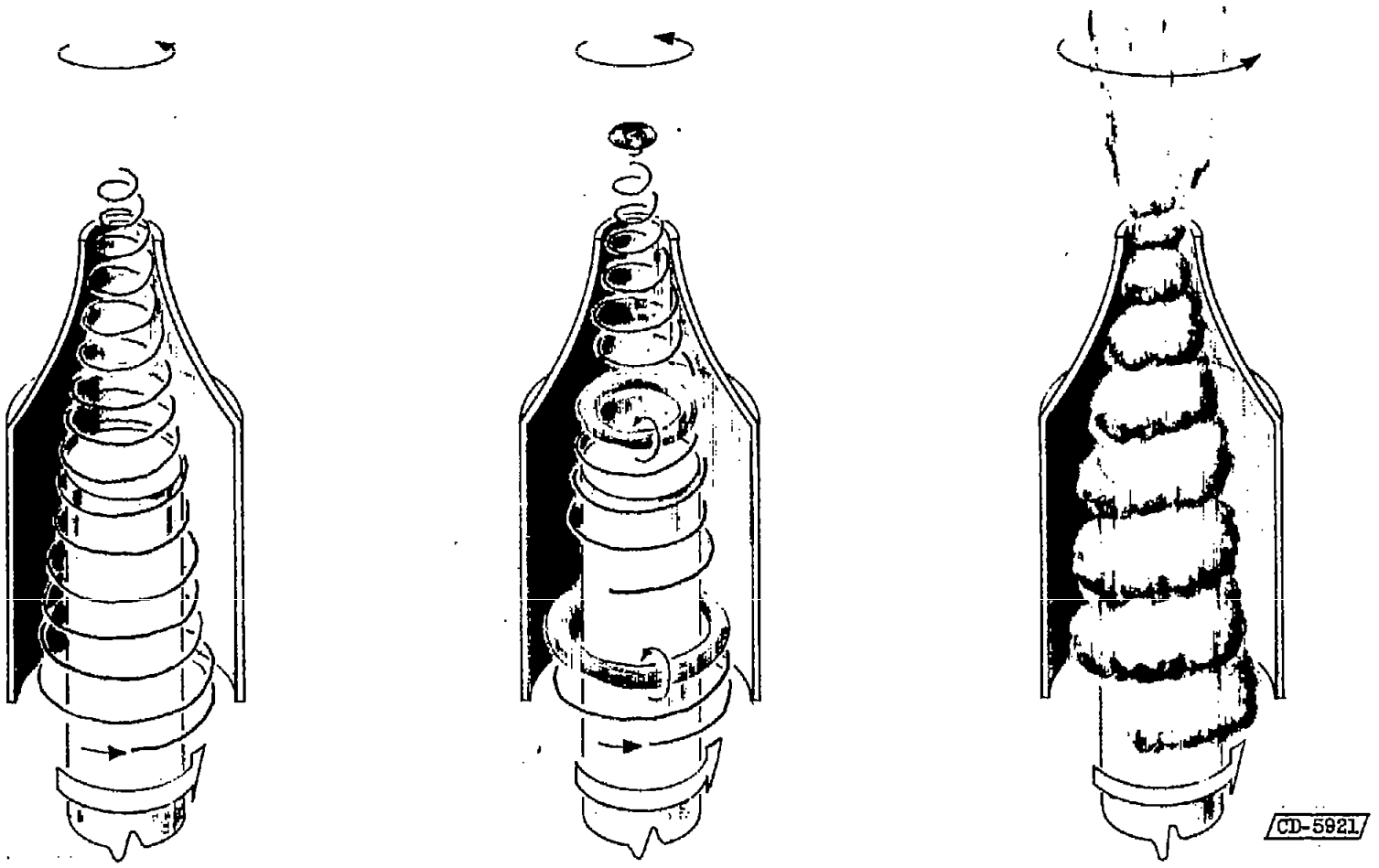

Centerbody speed, rpm ≈ 25 | ≈ 125 | > 300

Figure 3. - Flow regions of gas.

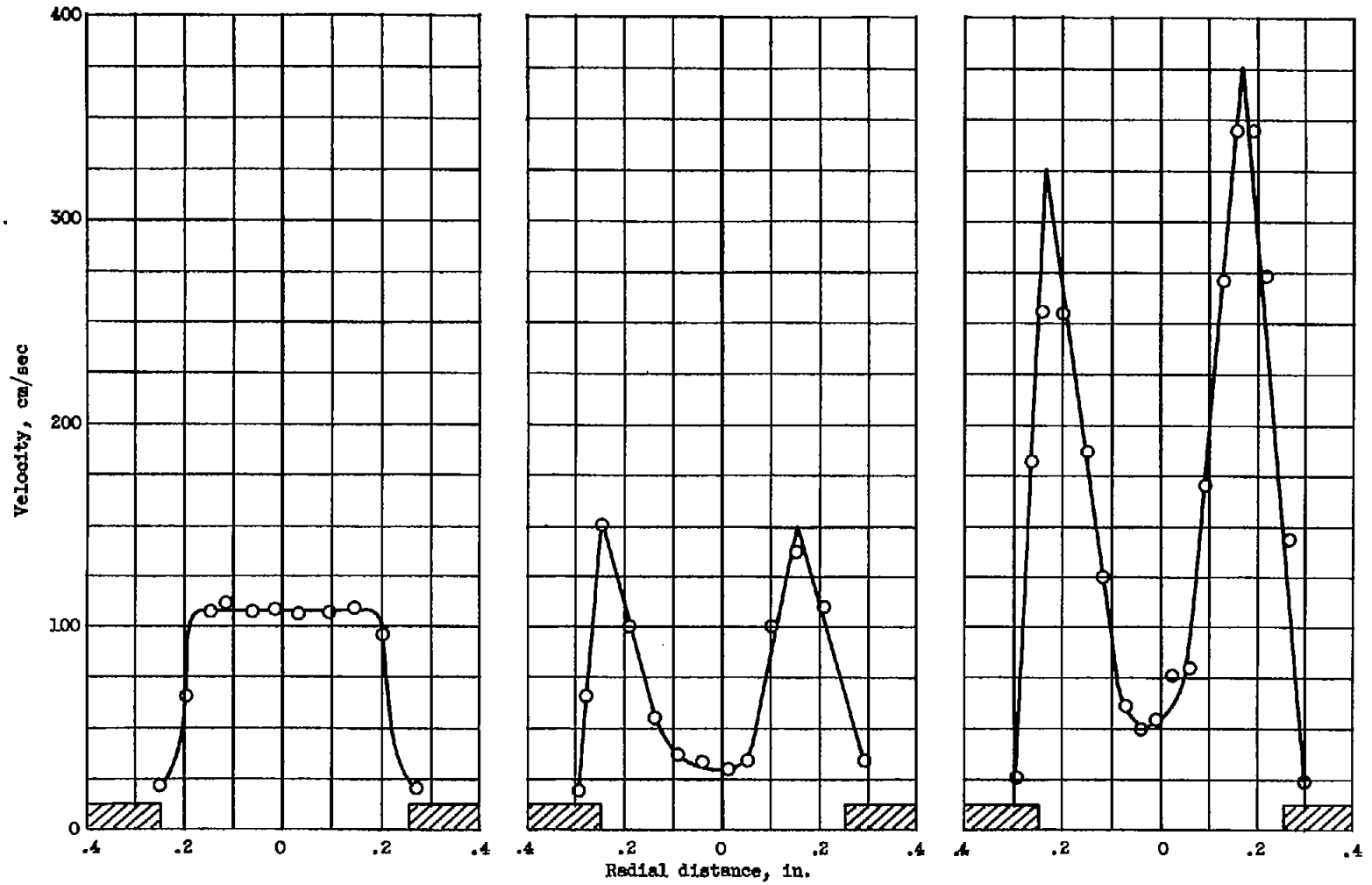

(a) Axial velocity; centerbody motionless.

(b) Axial velocity; centerbody at 205 rpm.

(c) Vortex velocity; centerbody at 205 rpm.

Figure 4. - Effect of centerbody rotation on velocity profile 3.5 millimeters above nozzle.

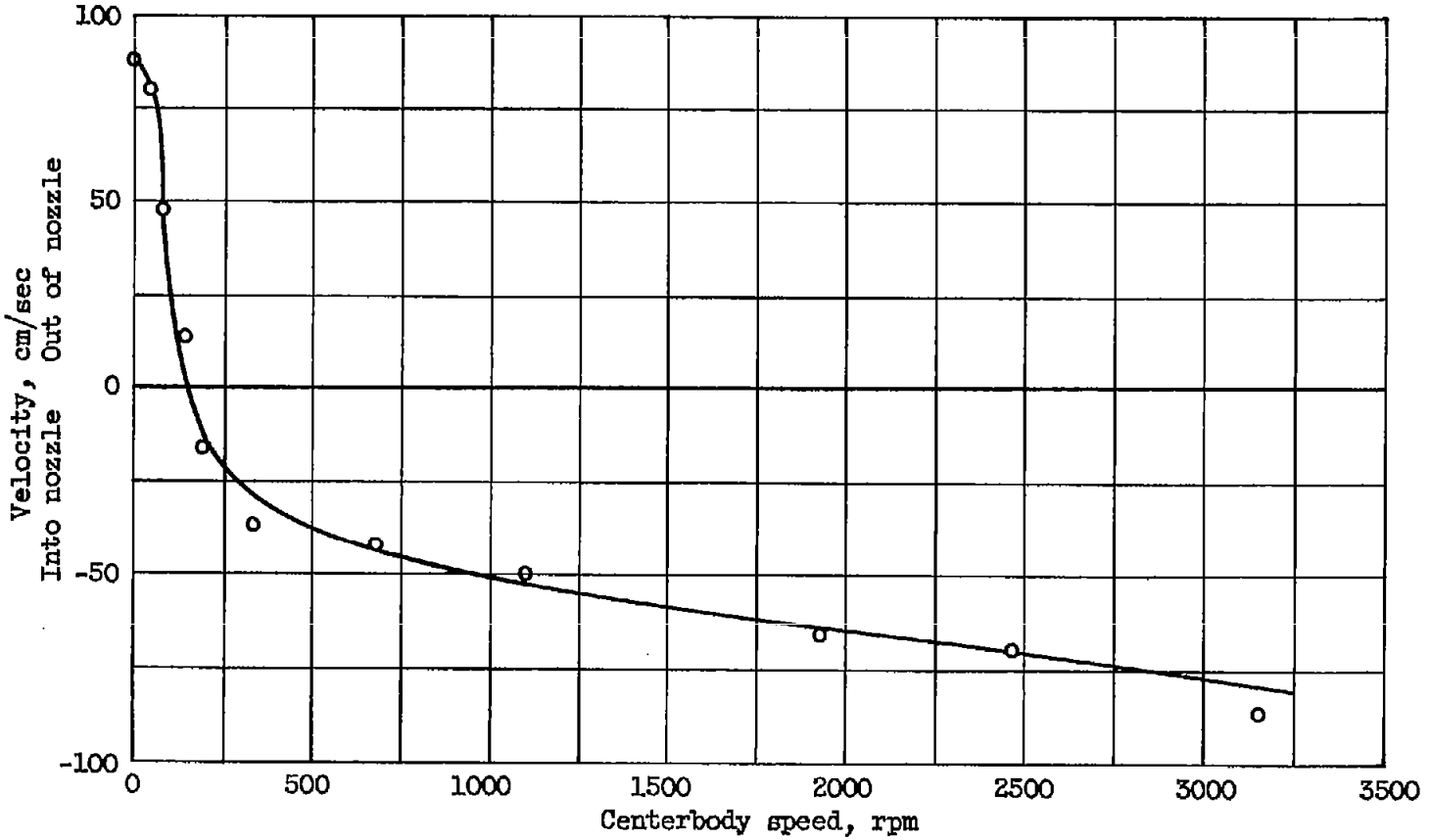

Figure 5. - Velocity at nozzle axis as a function of centerbody speed. Wire normal to axis located 3.5 millimeters above port. Flow rate, 90 cubic centimeters per second.

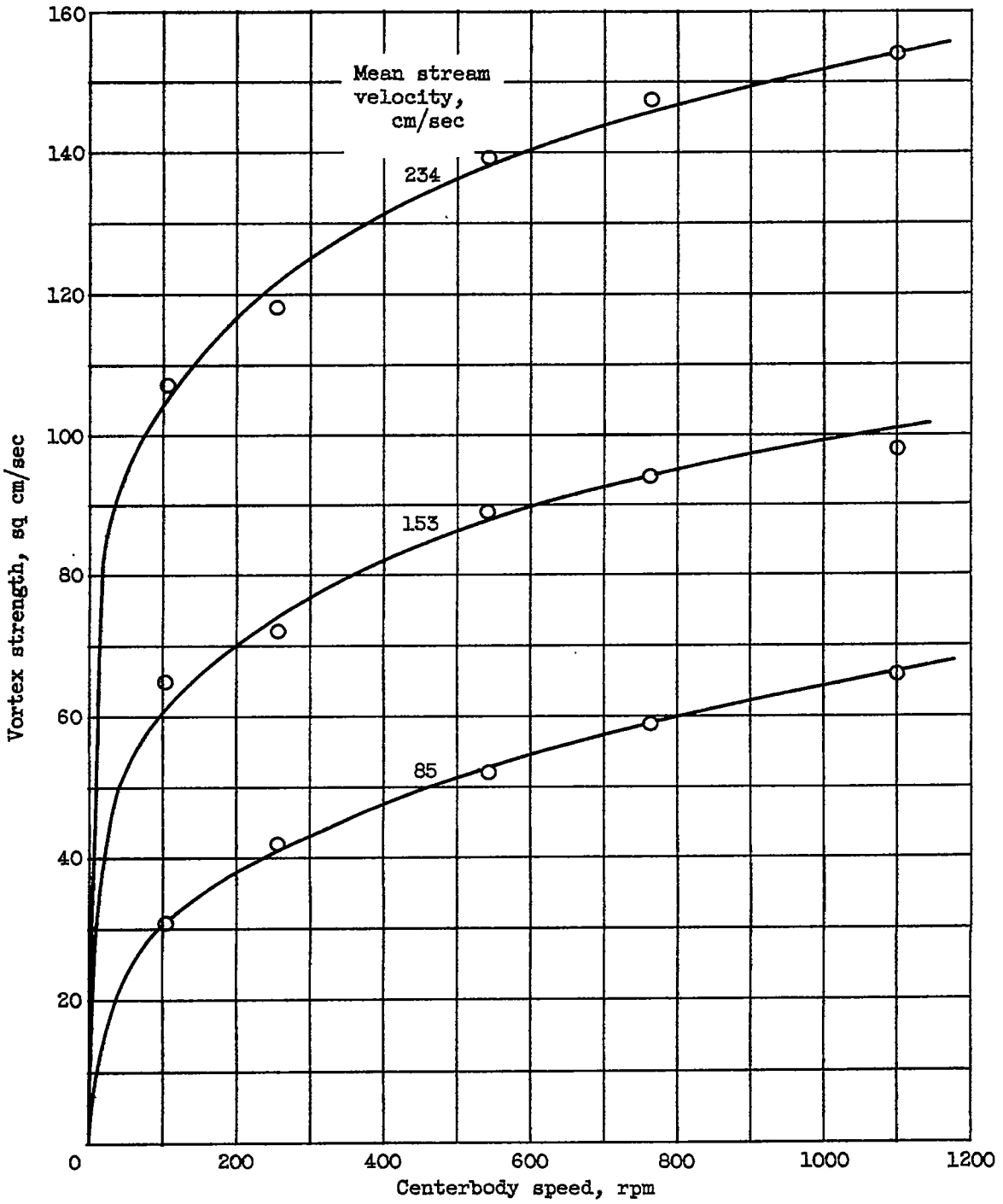

Figure 6. - Vortex strength as a function of centerbody speed and mean stream velocity.

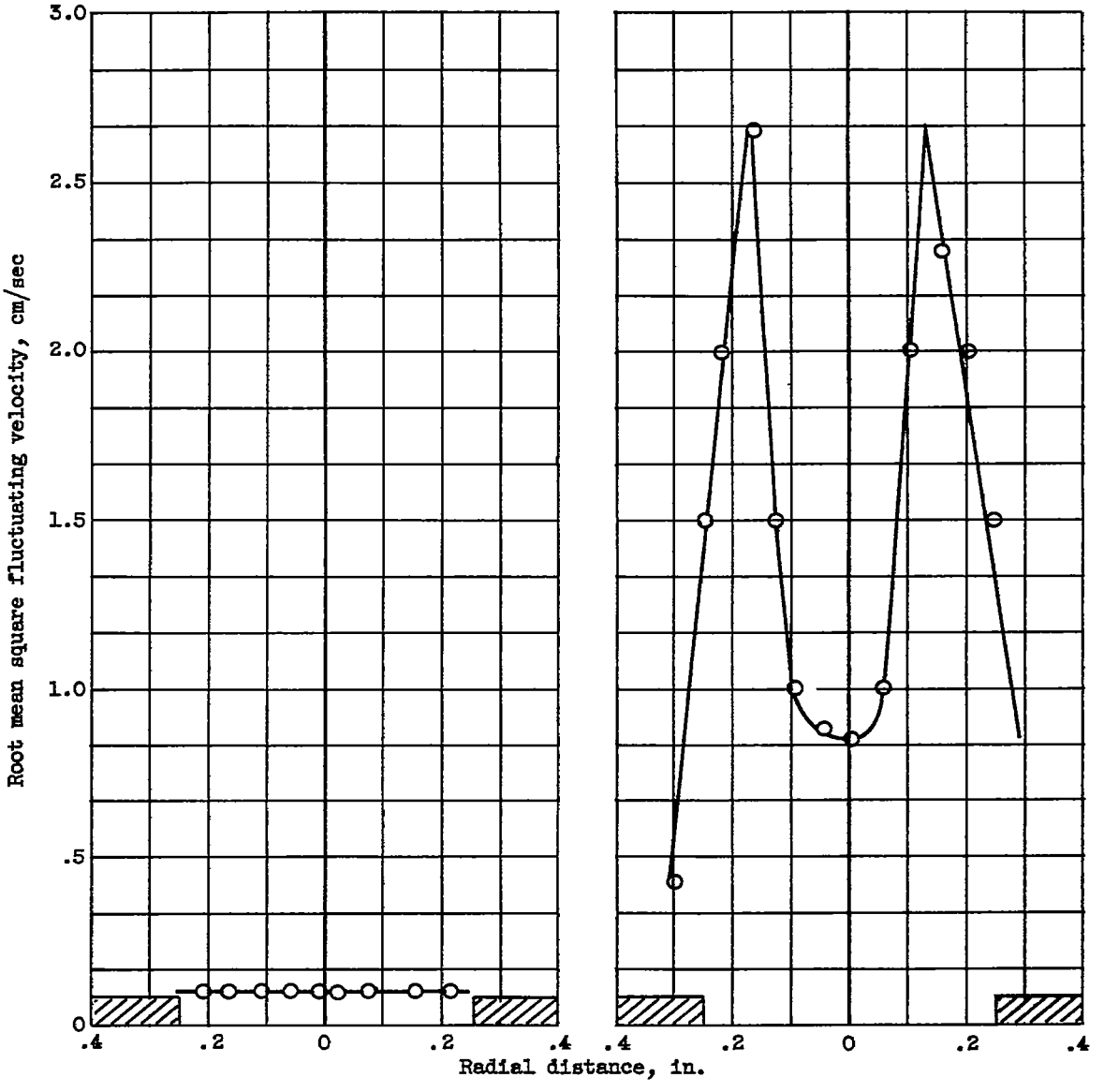

(a) Centerbody motionless. (b) Centerbody at 205 rpm.

Figure 7. - Effect of centerbody rotation on the production and distribution of turbulence intensity 3.5 millimeters above nozzle.

(a) Vortex strength, 0 centimeters squared per second.

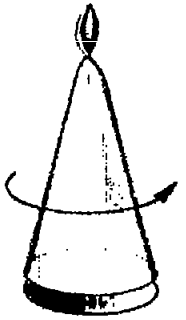

(b) Vortex strength, ≈ 10 centimeters squared per second.

(c) Vortex strength, ≈ 20 centimeters squared per second.

(d) Vortex strength, ≈ 30 to 60 centimeters squared per second.

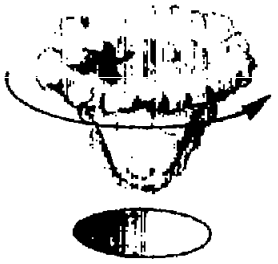

(e) Vortex strength, ≈ 60 centimeters squared per second.

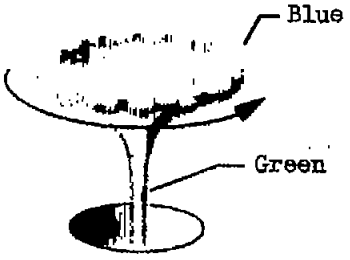

(f) Vortex strength, ≈ 200 centimeters squared per second; equivalence ratio, ≈ 1.5.

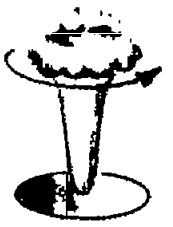

CD-5920

(g) Vortex strength, ≈ 200 centimeters squared per second; equivalence ratio, ≈ 0.7.

Figure 8. - Flame shapes at various vortex strengths.

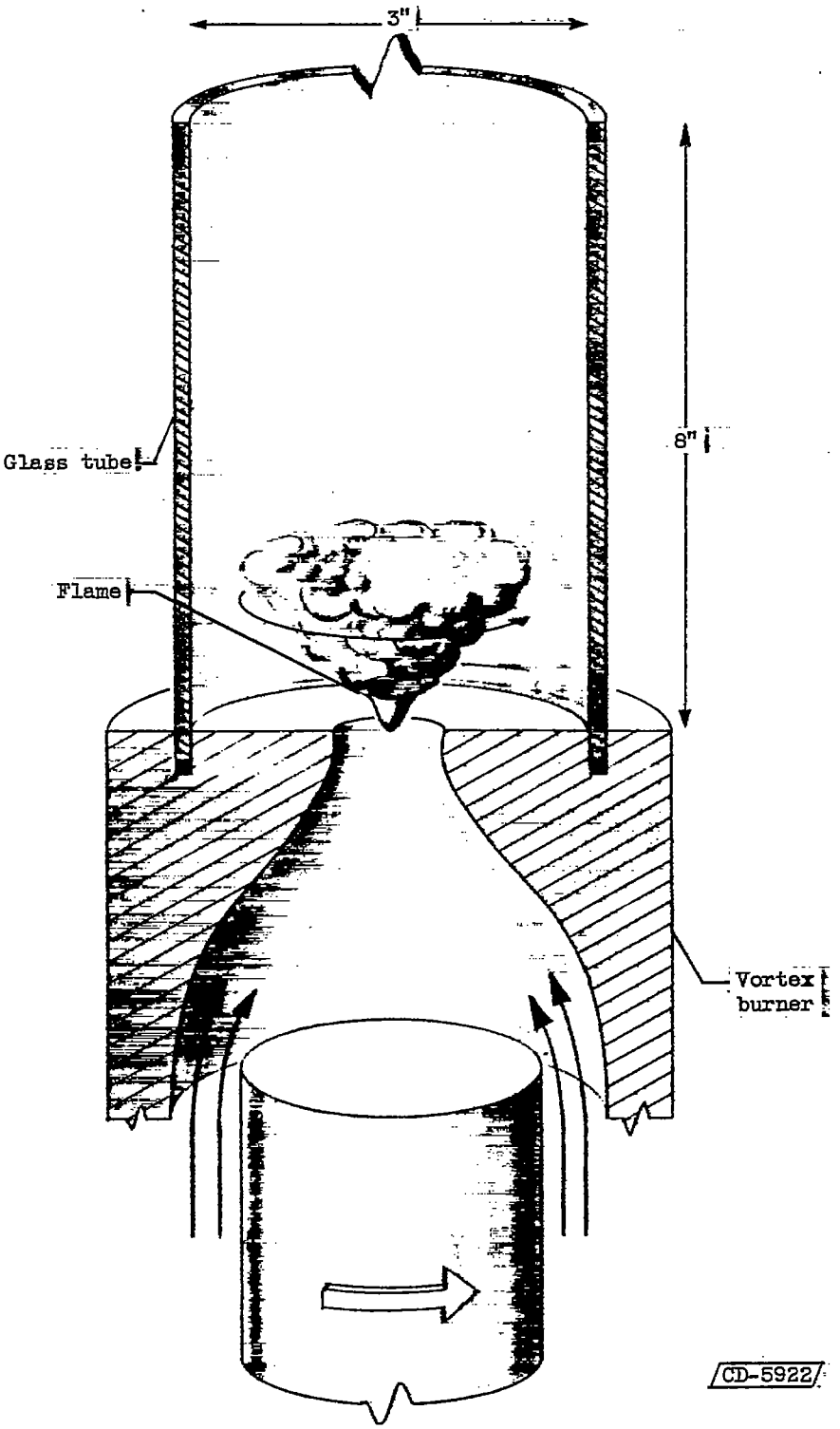

Figure 9. - Experimental arrangement to prevent access of ambient air to vortex flame.

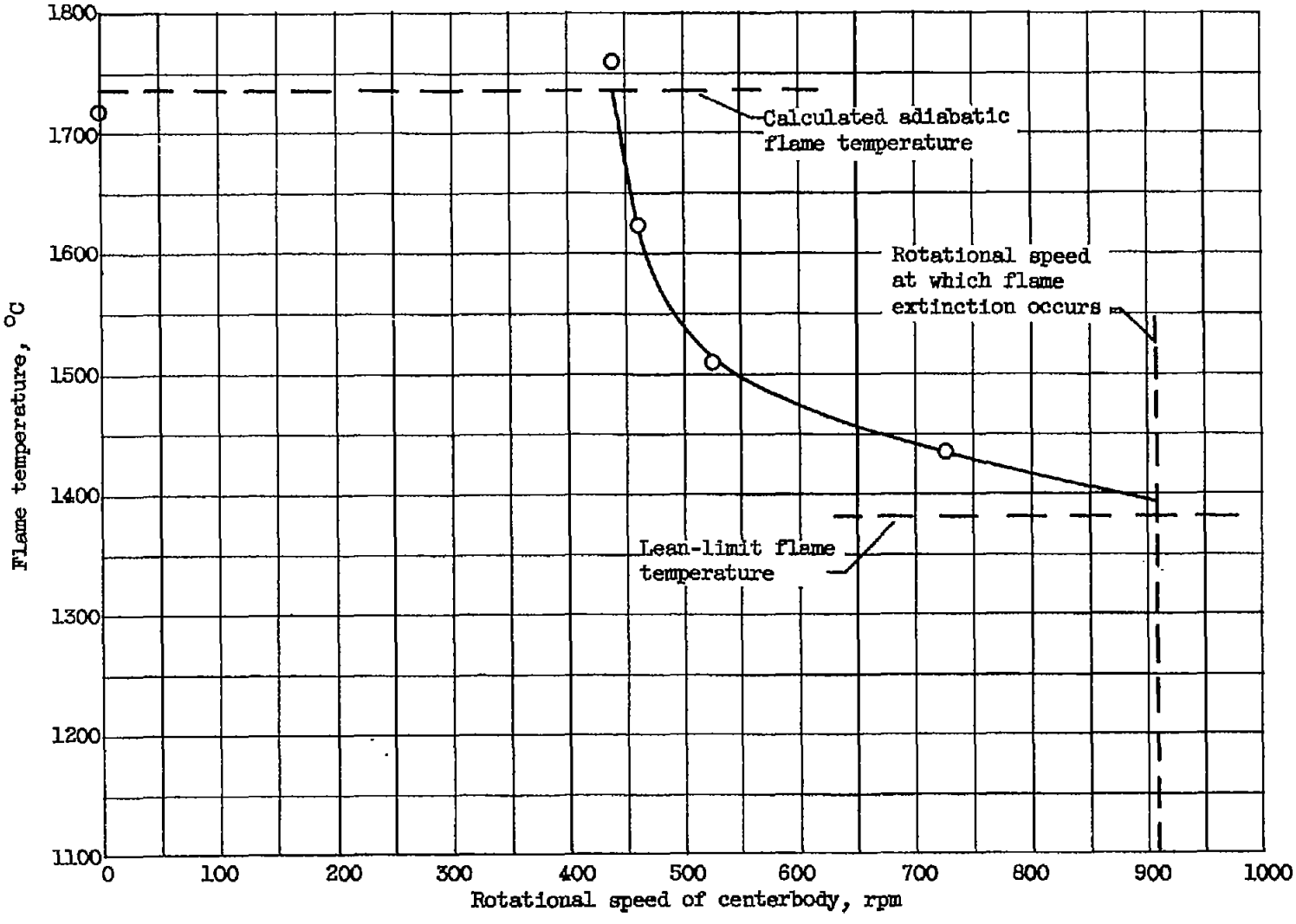

Figure 10. - Temperature of recirculation zone of a lean (3.1 percent propane) flame in strong vortex flow. Mean flow velocity, 396 centimeters per second.

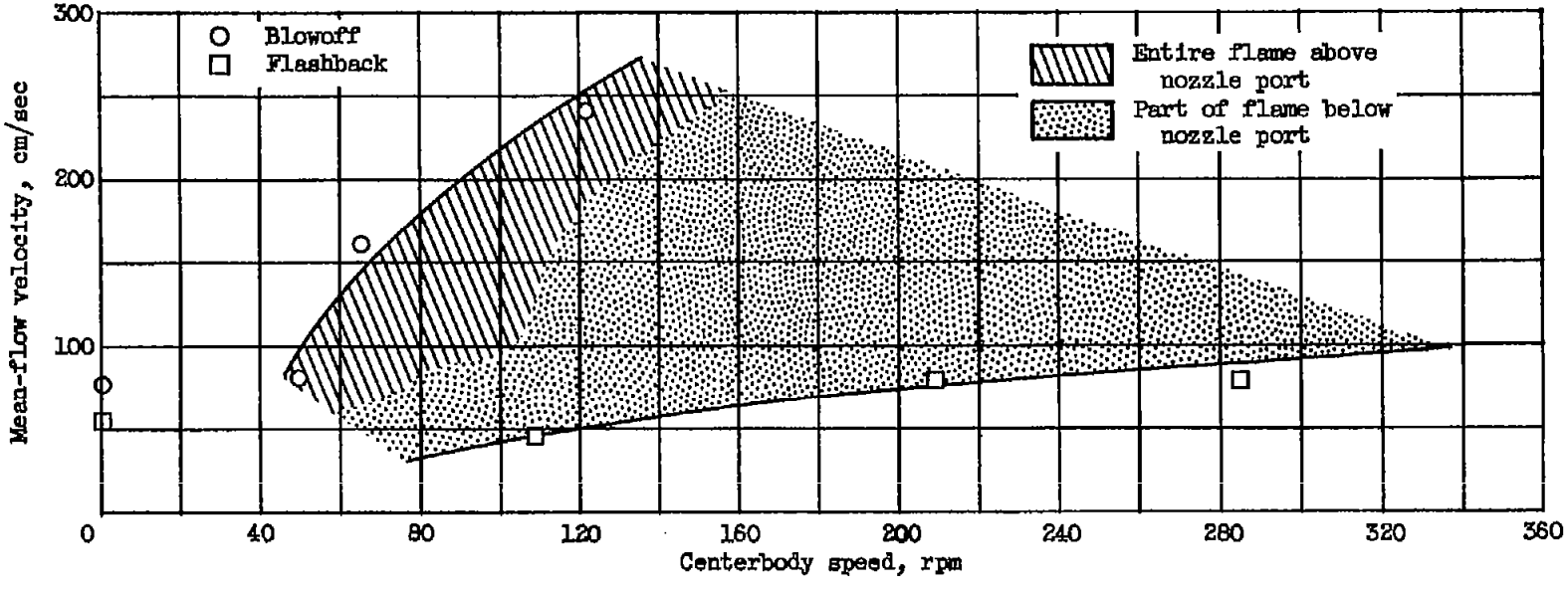

(a) 3 Percent propane.

Figure 11. - Stability limits for propane-air flames.

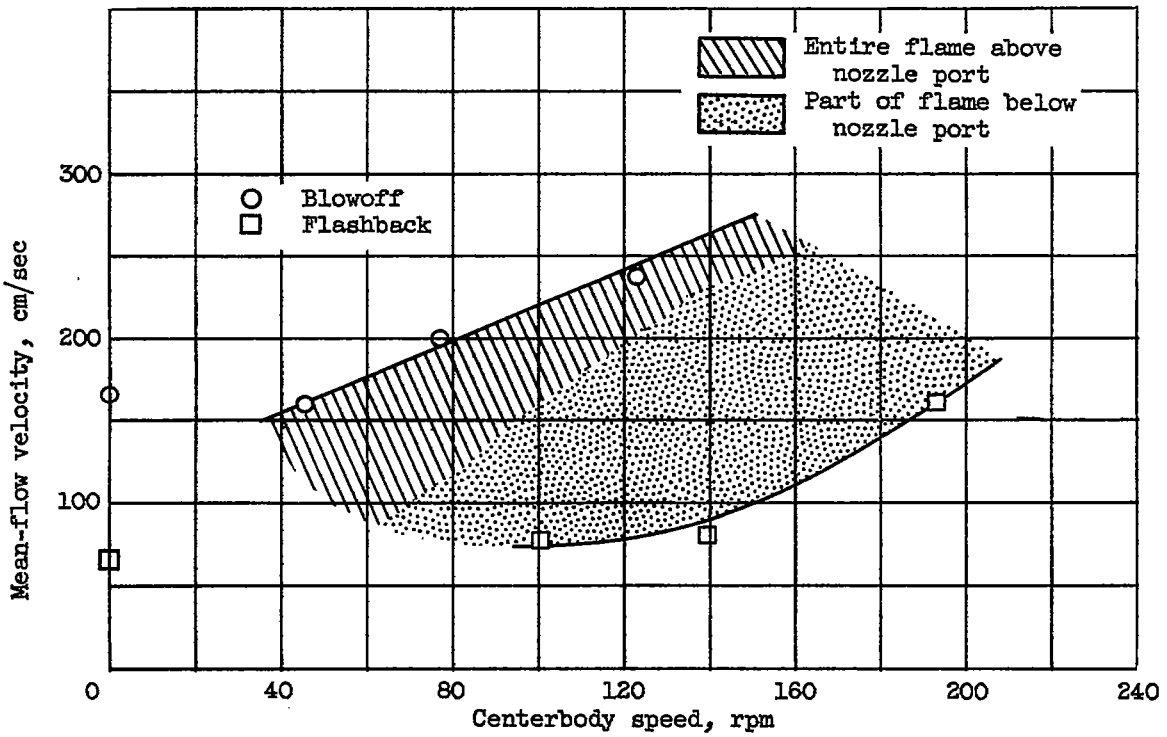

(b) 3.5 Percent propane.

Figure 11. - Continued. Stability limits for propane-air flames.

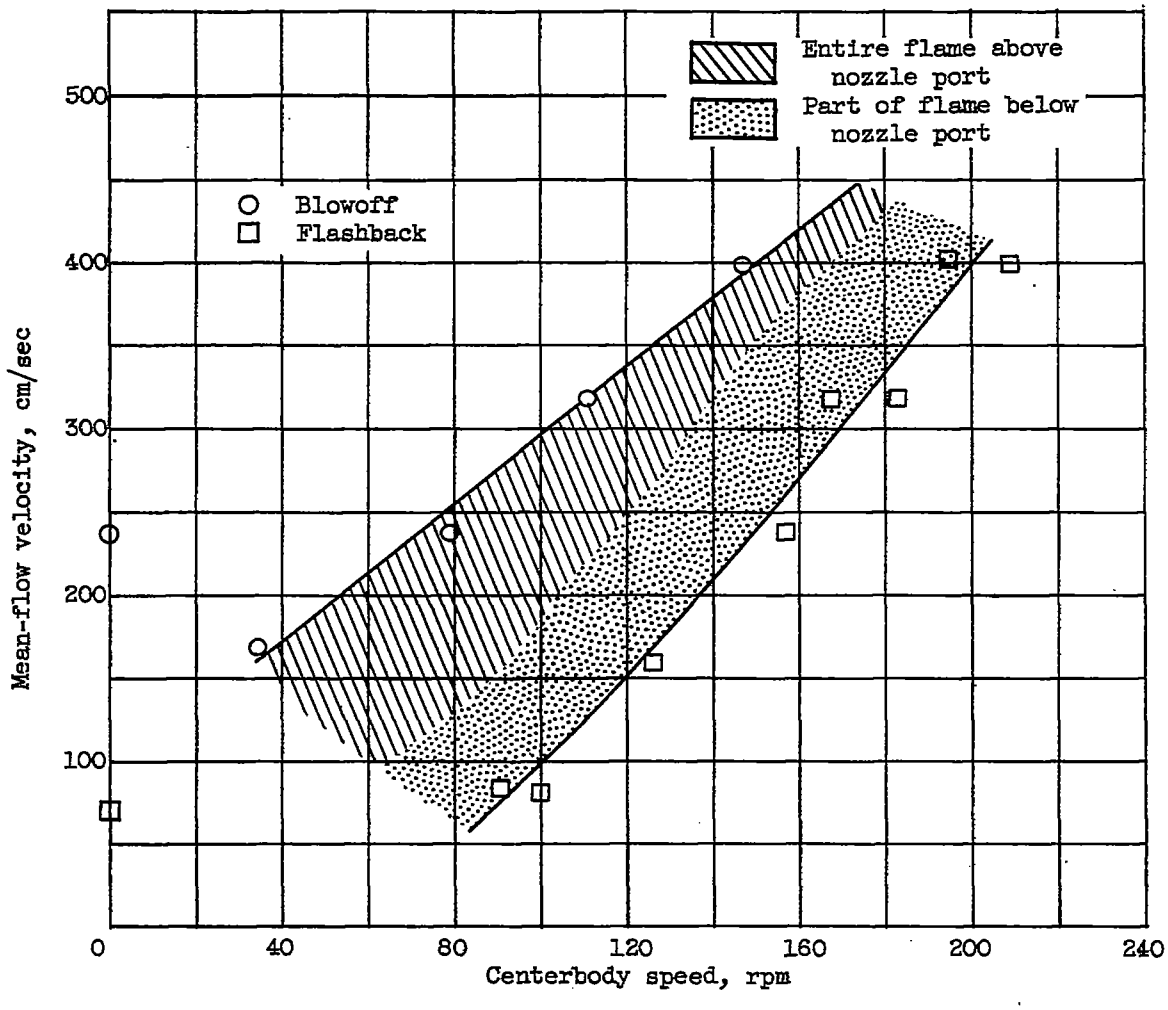

(c) 4 Percent propane.

Figure 11. - Continued. Stability limits for propane-air flames.

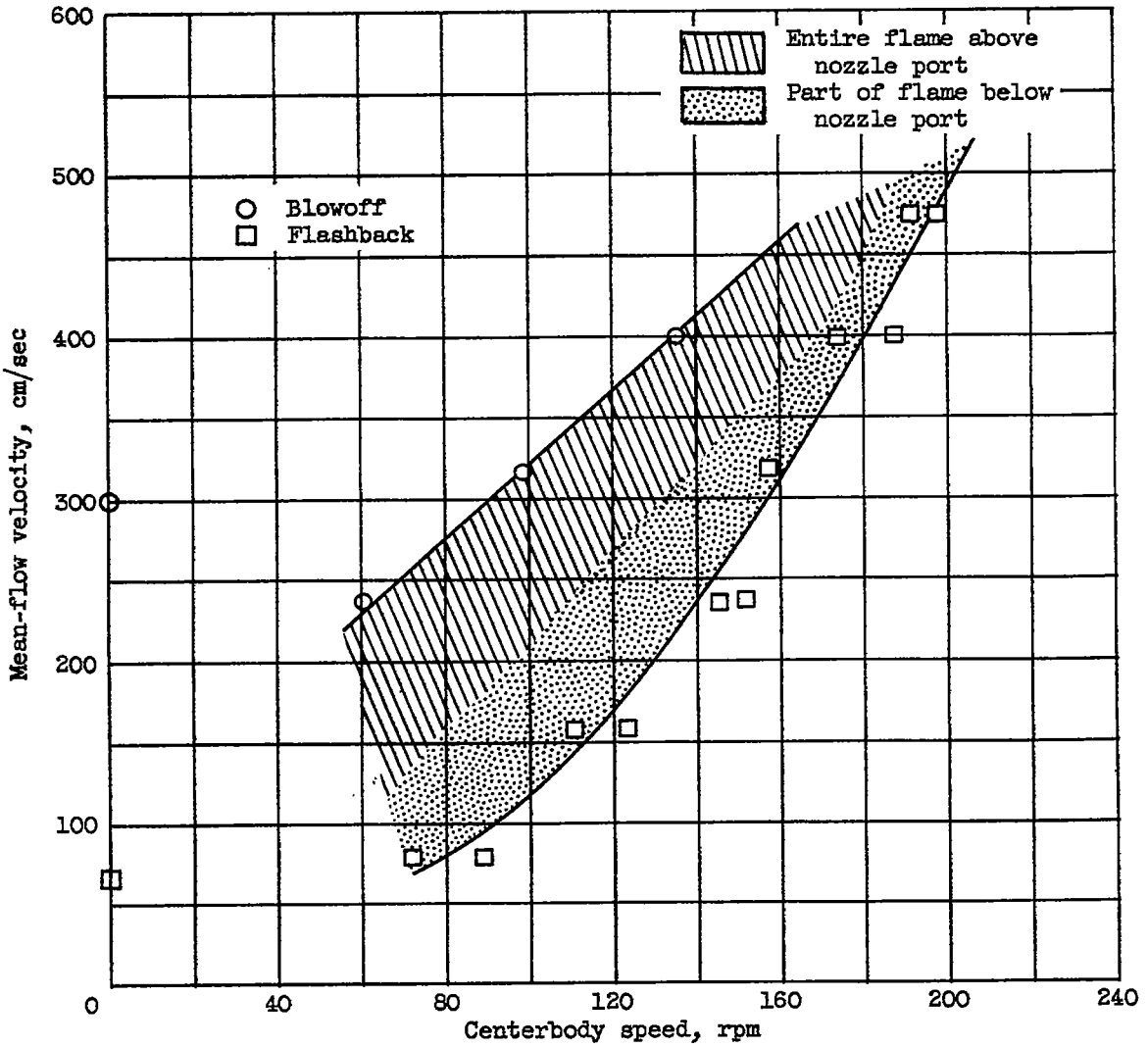

(d) 4.5 Percent propane.

Figure 11. - Continued. Stability limits for propane-air flames.

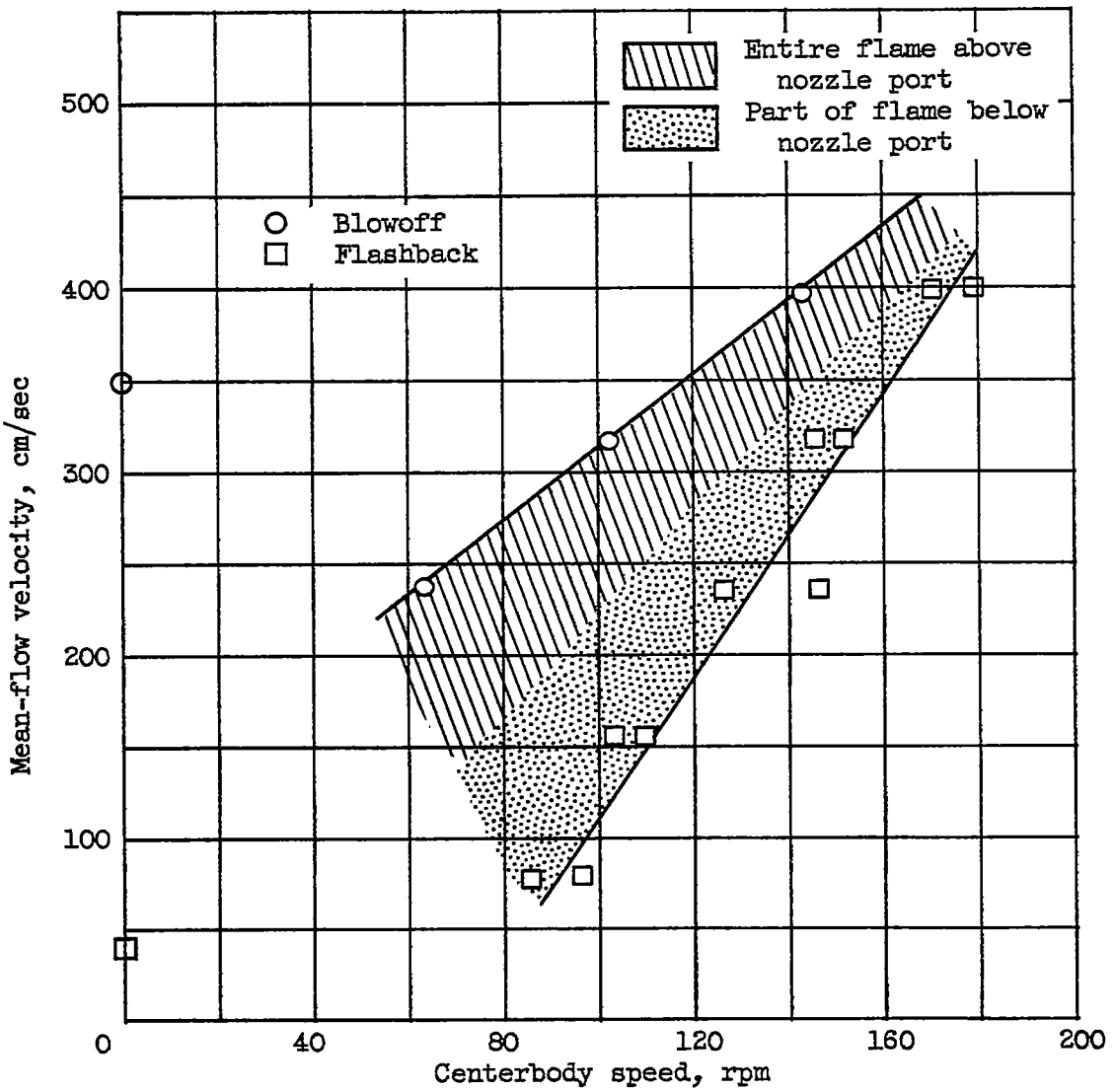

(e) 5.0 Percent propane.

Figure 11. - Concluded. Stability limits for propane-air flames.

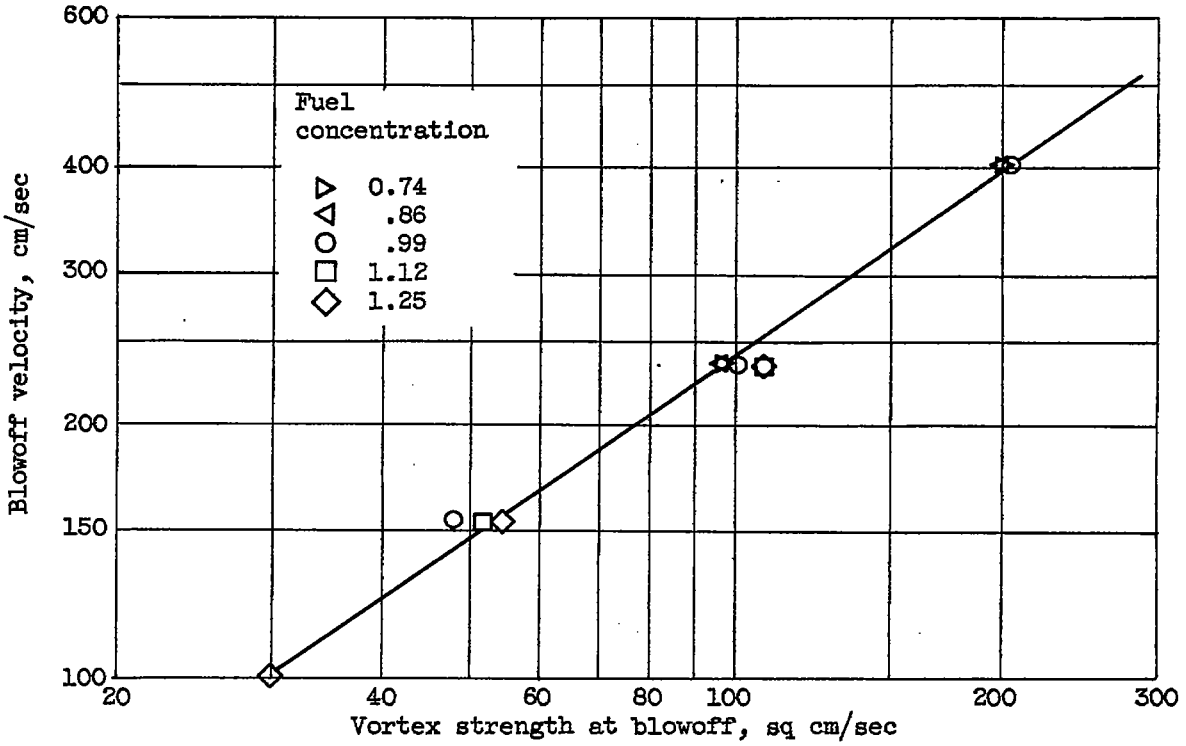

Figure 12. - Effect of vortex strength on blowoff velocity at various fuel concentrations.

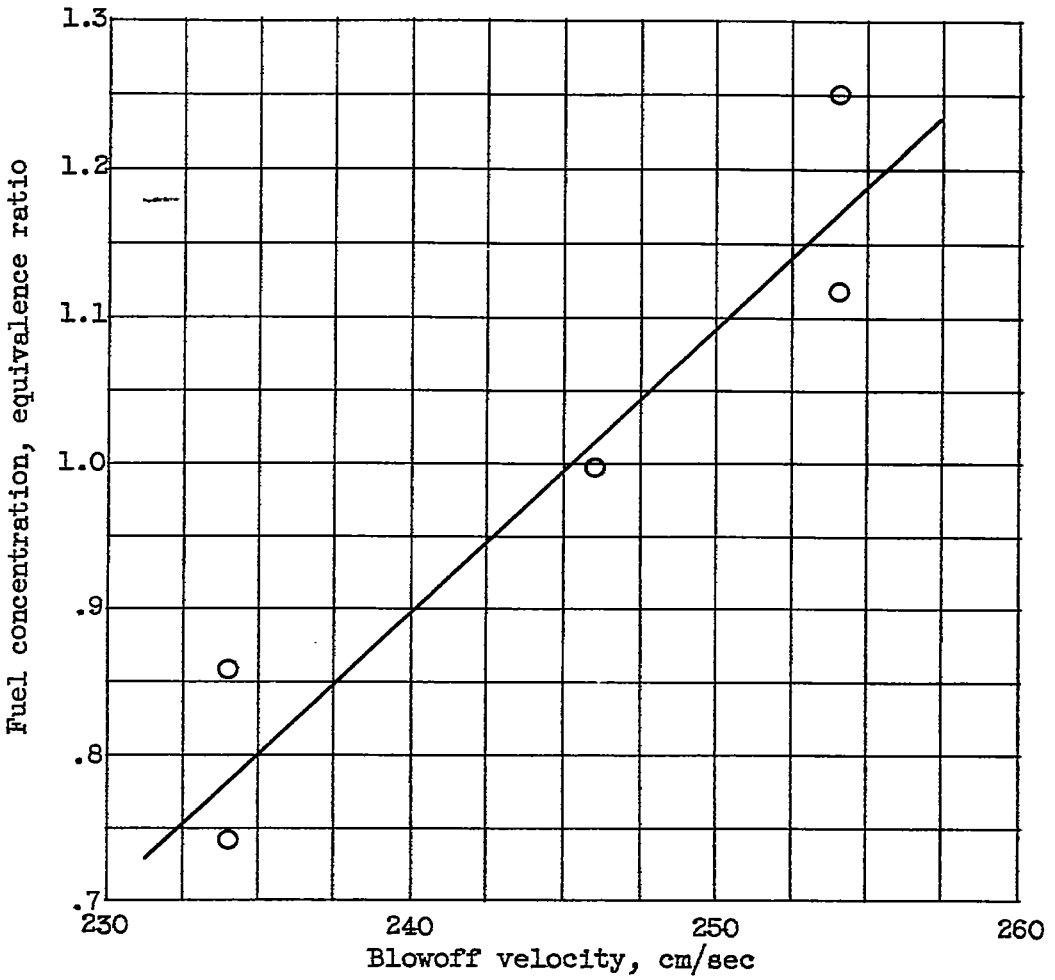

Figure 13. - Effect of equivalence ratio on blowoff velocity at constant vortex strength of 108 square centimeters per second.